Spontaneous motion of localized structures induced by parity symmetry breaking transition

A. J. Alvarez-Socorro,[1] M. G. Clerc,[1] and M. Tlidi[2]
[1]*Departamento de Física and Millennium Institute for Research in Optics, FCFM, Universidad de Chile, Casilla 487-3, Santiago, Chile*
[2]*Département de Physique, Université Libre de Bruxelles (U.L.B.), CP 231, Campus Plaine, Bruxelles 1050, Belgium*

(Received 15 December 2017; accepted 7 May 2018; published online 29 May 2018)

We consider a paradigmatic nonvariational scalar Swift-Hohenberg equation that describes short wavenumber or large wavelength pattern forming systems. This work unveils evidence of the transition from stable stationary to moving localized structures in one spatial dimension as a result of a parity breaking instability. This behavior is attributed to the nonvariational character of the model. We show that the nature of this transition is supercritical. We characterize analytically and numerically this bifurcation scenario from which emerges asymmetric moving localized structures. A generalization for two-dimensional settings is discussed. *Published by AIP Publishing.*
https://doi.org/10.1063/1.5019734

The formation of localized structures (LSs) often called cavity solitons or dissipative solitons is a universal feature of the self-organized non-equilibrium systems and is of common occurrence in many fields of nonlinear science ranging from biology, chemistry, to physics. The important issue of our analysis is to reveal the transition from a stationary to moving localized structures that may occur in practical systems. We show that an internal parity symmetry breaking bifurcation allows localized structures to move in an arbitrary direction. We illustrate this bifurcation scenario in the paradigmatic nonvariational Swift-Hohenberg equation that has been derived for many far from equilibrium systems. These results are obtained in the particular limit of nascent bistability and large wavelength or small wavenumber pattern forming regime. Therefore, the present analysis could be applied to more realistic models. Understanding the dynamics of localized structures may allow for the manipulation and the control of light in advanced optical devices.

I. INTRODUCTION

Localized structures (LS's) have been theoretically predicted and experimentally observed in many fields of nonlinear science, such as laser physics, hydrodynamics, fluidized granular matter, gas discharge system, and biology.[1–10] These solutions correspond to a portion of the pattern surrounded by regions in the homogeneous steady state. However, localized structures are not necessarily stationary. They can move or exhibit a self-pulsation as a result of *external* symmetry breaking instability induced by a phase gradient,[11] off-axis feedback,[12] resonator detuning,[13] and space-delayed feedback.[14] This motion has also been reported using a selective[15,16] or a regular time-delay feedbacks.[17]

We identify an internal symmetry breaking instability that causes a spontaneous transition from stationary to moving localized structures in nonvariational systems. In contrast, variational systems, i.e., dynamical systems characterized by a functional, an internal symmetry breaking instability causes the emergence of motionless asymmetric localized states.[19,20] To investigate this nonvariational transition, we consider a generic nonvariational scalar Swift-Hohenberg equation. This is a well-known paradigm in the study of spatial periodic and localized patterns. It has been derived for that purpose in liquid crystal light valves with optical feedback,[21,22] in vertical cavity surface emitting lasers,[23] and in other fields of nonlinear science.[24] Generically, it applies to systems that undergo a Turing-Prigogine instability, close to a second-order critical point marking the onset of a hysteresis loop. This equation reads

$$\partial_t u = \eta + \mu u - u^3 - \nu\nabla^2 u - \nabla^4 u + 2bu\nabla^2 u + c(\nabla u)^2. \tag{1}$$

The real order parameter $u = u(x, y, t)$ is an excess field variable measuring the deviation from criticality. Depending on the context in which Eq. (1) is derived, the physical meaning of the field variable u can be the electric field, biomass, molecular average orientation, or chemical concentration. The control parameter η measures the input field amplitude, the aridity parameter, or the chemical concentration. The parameter μ is the cooperativity, and ν is the diffusion coefficient. The Laplace operator $\nabla^2 \equiv \partial_{xx} + \partial_{yy}$ acts on the plane (x, y). The parameters b and c measure the strength of nonvariational effects. The terms proportional to c and b, respectively, account for the nonlinear advection and nonlinear diffusion, which in optical systems can be generated by the free propagation of feedback light.[21,22]

For $b = c$, Eq. (1) is variational,[24] i.e., the model reads $\partial_t u = -\delta F(u)/\delta u$, with $F(u)$ being the free energy or the Lyapunov functional. In this case, any perturbation compatible with boundary conditions evolves toward either a homogeneous or inhomogeneous (periodic or localized) stationary states corresponding to a local or global minimum of $F(u)$.

Therefore, complex dynamics such as time oscillations, chaos, and spatiotemporal chaos are not allowed in the limit $b = c$. In particular, in this regime, stationary localized structures and localized patterns have been predicted.[25] An example of a stationary LS in one-dimension is shown in the left panel of Fig. 1. The obtained localized structure has a maximum value of field $u(x, t)$ located at the position x_0. The stationary LS has been studied for Eq. (1) in one dimensional (1D) spatial coordinate, as well their snaking bifurcation diagram.[26,27] When $b \neq c$, the model equation losses its variational structure and allows for the mobility of unstable asymmetric localized structures, *rung states*, that connect the symmetric states.[26] Indeed, the system exhibits a drift instability leading to the motion of localized structures in an arbitrary direction. However, these states are unstable states for small nonvariational coefficients.

In this paper, we characterize the transition from stable stationary to moving localized structures in non-variational real Swift-Hohenberg equation. Figure 1 illustrates stable moving localized structures. We show that there exists a threshold over which a single LS starts to move in an arbitrary direction since the system is isotropic in both spatial directions. We compute analytically and numerically the bifurcation diagram associated with this transition. In one dimensional setting, the transition is always supercritical within the range of the parameters that we explore. The threshold and the speed of LS is evaluated both numerically and analytically. In two-dimensional settings, numerical simulations of the governing equation indicate that the nature of the transition towards the formation of moving localized bounded states is not a supercritical bifurcation. It is worth to mention another type of internal mechanism that occurs in regime devoid of patterns and may lead to a similar phenomenon for fronts propagation through a non-variational Ising Bloch transition.[19,28–30] The Ising-Bloch transition has been first studied in the context of magnetic walls.[19] Soon after, it has been considered in a various out of equilibrium systems such as driven liquid crystal,[29] coupled oscillators,[30] and nonlinear optic cavity.[31] More recently, it has been shown that non-variational terms can induce propagation of fronts in quasi-one-dimensional liquid crystals based devices.[32] Experimental observation of a supercritical transition from stationary to moving localized structures has been realized in two-dimensional planar gas-discharge systems.[33]

The paper is organized as follows: the numerical characterization of the bifurcation scenarios triggered by an internal symmetry breaking instability leading to the formation of asymmetric traveling localized structures is discussed in Sec. II. At the end of this section, we perform numerical simulations in one-dimensional system Eq. (1). In Sec. III, we perform an analytical analysis of the symmetry breaking instability. Two-dimensional moving bounded localized structures are analyzed, and their bifurcation diagram is determined in Sec. IV. Finally, the conclusions are presented in Sec. V.

II. NUMERICAL CHARACTERIZATION OF PARITY BREAKING TRANSITION

We investigate the model Eq. (1) numerically in the case where $b \neq c$ in 1D with periodic boundary conditions. The results are summarized in the bifurcation diagram of Fig. 1. We fix all parameters and we vary the nonvariational parameter c. When increasing the parameter $c < c^*$, LS's are stationary. There exist a threshold $c = c^*$ at which transition from stationary to moving LS's takes place. This transition is supercritical. For $c > c^*$, stationary LS becomes unstable, and the system undergoes a bifurcation towards the formation of moving localized structures. The direction in which LS propagates depends on the initial condition used. Indeed, there is no preferred direction since the system is isotropic. The spatial profiles of the stationary and the moving localized states are shown in Fig. 2. The shadow regions allow emphasizing the symmetric (stationary) and asymmetric (moving) solutions concerning the localized structure position. We clearly see from this figure that stationary LS is

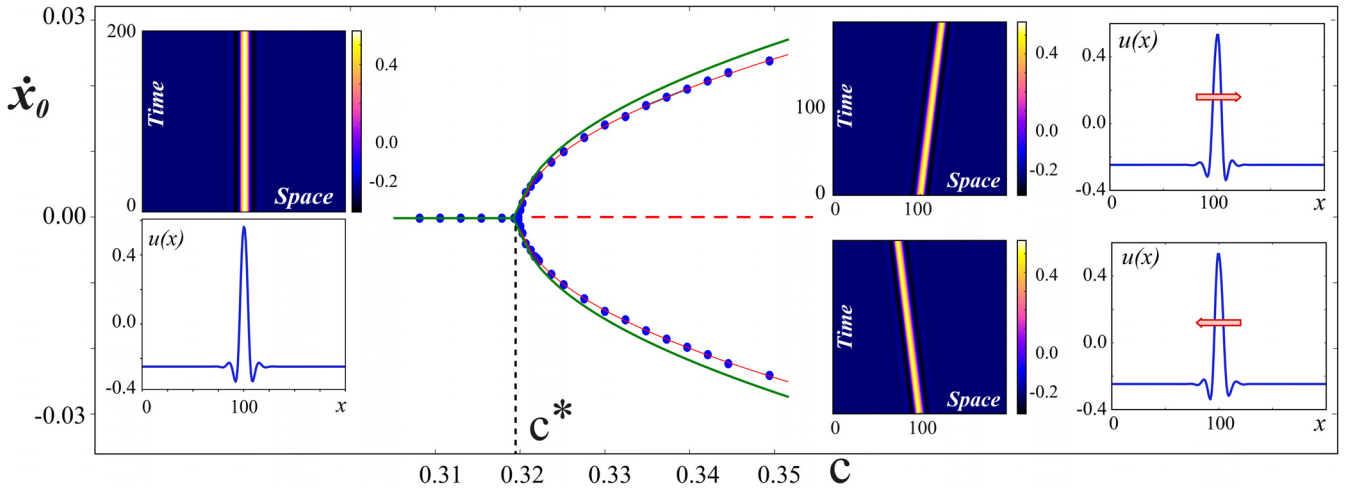

FIG. 1. The speed of localized structure $v = \dot{x}_0$ as a function of the parameter c. At the transition point, $c \equiv c^* \approx 0.319$. Dots indicate localized structures speed obtained from numerical simulations of Eq. (1). Green curves are associated with the analytical results depicted in Sec. III and red curves are associated with the fit of the numerical values given by: $v = \dot{x}_0 = 0.1467\sqrt{c - 0.319}$. Parameters are $\mu = \eta = -0.02$, $\nu = 1$, and $b = -0.9$. Left insets account for the profile and the spatiotemporal evolution of a motionless localized structure. Right top (bottom) insets account for the profile and the spatiotemporal evolution of a right (left) moving localized structure.

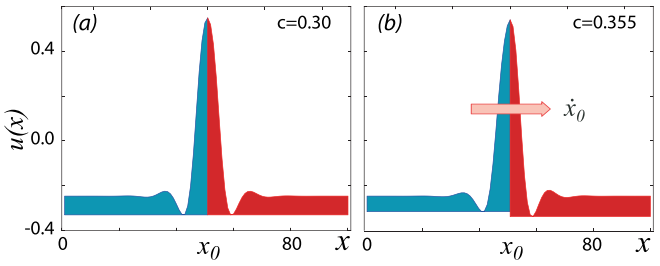

FIG. 2. Profile of localized structures obtained from numerical simulations of Eq. (1). Parameters are $\mu = \eta = -0.02$, $\nu = 1$, and $b = -0.9$. (a) Stationary and (b) moving localized structure.

symmetric concerning its maximum. This can be explained by the fact that a spontaneous spatial parity breaking symmetry accompanies the transition from stationary to moving localized structures. In fact, if the parity with respect to its position $\int_{x_0-L}^{x_0+L} u(x,t)dx$ is positive (negative), it moves to the right (left).

We have measured the speed of moving LS solutions of Eq. (1) numerically, by varying both c and b parameters. The results are summarized in Fig. 3. There are three different dynamical regimes. When increasing both parameters b and c, the stationary localized structures are stable in the range delimited by the curve Γ_1. These structures exhibit a spontaneous motion leading to the formation of moving LSs solutions in the range of parameters delimited by the curves Γ_1 and Γ_2. By exploring the parameter space (b, c), we see clearly from Fig. 3 that the bifurcation towards the formation of moving LSs remains supercritical.

After the numerical characterization, we perform an analytical analysis of the transition towards moving LS. For this purpose, let us consider the linear dynamics around

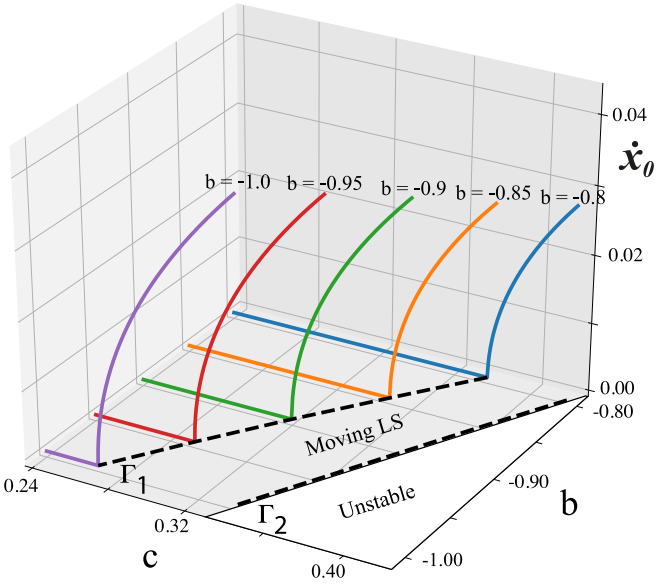

FIG. 3. The speed $v = \dot{x}_0$ as a function of the nonvariational parameters c and b obtained by numerical simulations of Eq. (1). Parameters are $\mu = \eta = -0.02$, and $\nu = 1$; for each curve, different fixed values of the parameter b are considered, which are indicated in the upper part of the respective curve. The two segmented curves (Γ_1, Γ_2) limit the region where moving localized structures are observed. The line Γ_1 marks the transition from stationary to moving localized structures.

stationary LS; $u_{ls}(x - x_0)$ located at $x = x_0$. The linear operator reads

$$\mathcal{L}\varphi \equiv \left[\mu - 3u_{ls}^2 - \nu\partial_{xx} - \partial_{xxxx} + 2bu_{ls}\partial_{xx}\right]\varphi + 2c(\partial_x u_{ls})\partial_x\varphi + 2b(\partial_{xx}u_{ls})\varphi. \quad (2)$$

Note that the operator $\mathcal{L}$ is not self-adjoint ($\mathcal{L} \neq \mathcal{L}^\dagger$). Due to the lack of analytical solutions of LS for Eq. (1), we compute numerically the spectrum and eigenvectors associated with $\mathcal{L}$, $\mathcal{L}^2$, and $\mathcal{L}^\dagger$. The spectrum of $\mathcal{L}$ always has an eigenvalue at the origin of the complex plane (the Goldstone mode) as shown in Fig. 4(a). The corresponding eigenfunction denoted by $|\chi_0\rangle \equiv \partial_z u_{ls}(x - x_0)$ is depicted in Fig. 4(a-i). When approaching the parity breaking transition threshold, another mode collides with the Goldstone mode as shown in Fig. 4(a). The corresponding eigenfunction of this mode is depicted in Fig. 4(a-ii). Note, however, that the profiles of both eigenfunctions are almost the same. At the threshold, these eigenfunctions are identical. This degenerate bifurcation has been reported in the Swift-Hohenberg equation with delayed feedback.[17,18] The spectrum of $\mathcal{L}^2$ operator is obtained by using the Jordan matrix decomposition as shown in Fig. 4(b). There are two eigenfunctions $|\chi_0\rangle$ and $|\chi_1\rangle = u_{as}(x - x_0)$, which satisfy

$$\begin{aligned} \mathcal{L}|\chi_1\rangle &= |\chi_0\rangle, \\ \mathcal{L}^2|\chi_1\rangle &= 0. \end{aligned} \quad (3)$$

The profiles of $|\chi_0\rangle$ and $|\chi_1\rangle$ are plotted in Figs. 4(b-i) and 4(b-ii), respectively. From this figure, we can see that for $|\chi_0\rangle$ mode, the integral $\int_{x_0-L}^{x_0+L} |\chi_0\rangle dx = 0$, while for $|\chi_1\rangle$ mode, the integral $\int_{x_0-L}^{x_0+L} |\chi_1\rangle dx \neq 0$. This indicate that the profile of $|\chi_1\rangle$ is asymmetric. This asymmetric mode has been reported in Refs. 19, 20, 26, 30, and 33. The eigenvalues and the critical eigenfunctions associated with the adjoint operator $\mathcal{L}^\dagger$ are depicted in Fig. 4(c).

Introducing the canonical inner product

$$\langle g|f\rangle = \int_{-\infty}^{\infty} f(x)g(x)dx \quad (4)$$

numerically, we have verified that critical modes are orthogonal $\langle\chi_0|\chi_1\rangle = 0$.

III. ANALYTICAL DESCRIPTION OF PARITY SYMMETRY BREAKING TRANSITION

To provide an analytical understanding of the parity symmetry breaking bifurcation, we focus our analysis on the one-dimensional setting. To do that, we explore the space-time dynamics in the vicinity of the critical point associated with the transition from stationary to moving LS at $c = c^*$ by defining a small parameter ϵ which measures the distance from that critical point as $c = c^* + \epsilon^2 c_0$. Our objective is to determine a slow time and slow space amplitude equations. We expand the variable $u(x, t)$ as

$$u(x,t) = u_{ls}(x - x_0(\epsilon t)) + \epsilon A'(\epsilon^2 t)u_{as}(x - x_0(\epsilon t)) + w(x, x_0, A'), \quad (5)$$

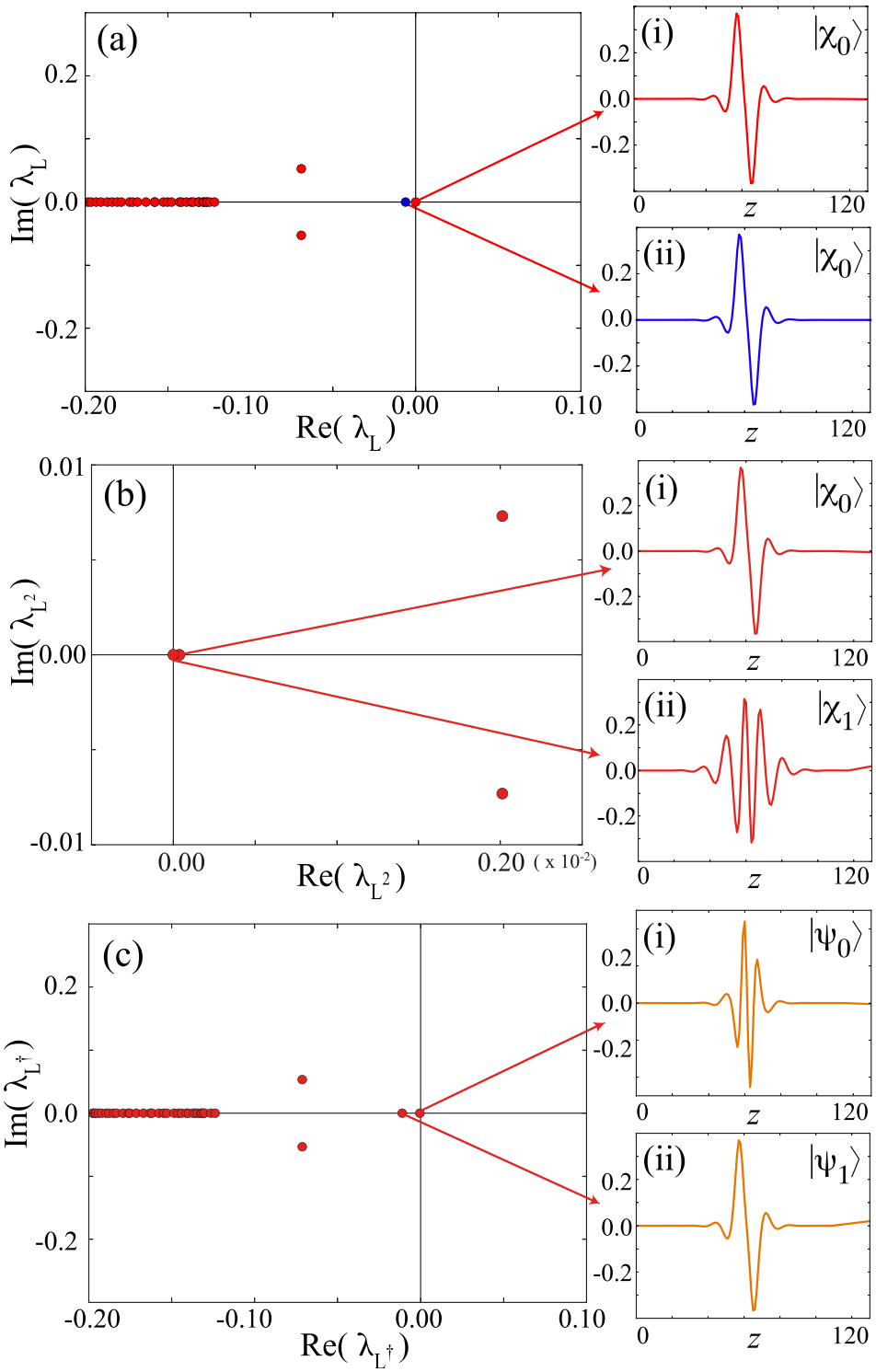

FIG. 4. Spectrum of linear operators. Real and imaginary parts of the eigenvalues associated with the linear operators (a) $\mathcal{L}$, (b) $\mathcal{L}^2$, and (c) $\mathcal{L}^\dagger$. Parameters are $\mu=-0.02$, $\nu=1.0$, $b=-0.9$, and $c=0.318$. Inset figures are the real part of the eigenfunction $|\chi_0\rangle$, $|\chi_1\rangle$, $|\psi_0\rangle$, and $|\psi_1\rangle$ for the Goldstone and the asymmetric mode associated with the zero eigenvalue, respectively.

where $u_{ls}(x-x_0(\epsilon t))$ is the stationary localized structure, and x_0 stands for the position of the localized structure. We assume that this position evolves on the slow time scale ϵt. The function $u_{as}(x-x_0(\epsilon t))\equiv|\chi_1\rangle$ is the generalized eigenfunction corresponding to the asymmetric mode. The amplitude A' is assumed to evolve on a much slower tine scale $\epsilon^2 t$, and $w(x,x_0,A')$ is a small nonlinear correction function that follows the scaling $w\ll\epsilon A'\ll 1$. By replacing the above ansatz (5) in the corresponding one-dimensional model of Eq. (1) and linearized in w, after straightforward calculations we obtain

$$\begin{aligned}-\mathcal{L}|w\rangle=&\epsilon\dot{x}_0|\chi_0\rangle-\epsilon^3\dot{A}'|\chi_1\rangle+\ell\epsilon A'|\chi_1\rangle\\&+c_0\left[\partial_z u_{ls}|\chi_0\rangle+\epsilon^2A'^2\partial_z u_{as}\partial_z|\chi_1\rangle+2\epsilon A'\partial_z u_{as}|\chi_0\rangle\right]\\&-\epsilon^3A'^3u_{as}^2|\chi_1\rangle-3\epsilon^2A'^2u_{as}u_{ls}|\chi_1\rangle+c^*\epsilon^2A'^2\partial_z u_{as}\partial_z|\chi_1\rangle\\&+2b(\epsilon A')^2u_{as}\partial_{zz}|\chi_1\rangle,\end{aligned}\tag{6}$$

where we have introduced the notation $\dot{x}_0=\partial_t x_0$, $\dot{A}'=\partial_t A'$, $z\equiv x-x_0(t)$ that corresponds to the coordinate in the co-moving reference frame with speed $\dot{x}_0$, and $|w\rangle\equiv w(x,x_0,A',\epsilon)$.

At order ϵ, the solvability condition[34] reads

$$\dot{x}_0 = -A'. \tag{7}$$

To determine the equation of the amplitude A' of the asymmetric mode, we apply on Eq. (6) the linear operator $\mathcal{L}$ and we obtain

$$\begin{aligned}-\mathcal{L}^2|w\rangle = &-\epsilon^3\dot{A}'\mathcal{L}|\chi_1\rangle + c_0\mathcal{L}\partial_z u_{ls}|\chi_0\rangle + c(\epsilon A')^2\mathcal{L}\partial_z u_{as}\partial_z|\chi_1\rangle \\ &+ 2\Delta c\epsilon A'\mathcal{L}\partial_z u_{as}|\chi_0\rangle - (\epsilon A')^3\mathcal{L}u_{as}^2|\chi_1\rangle \\ &+ c^*(\epsilon A')^2\mathcal{L}\partial_z u_{as}\partial_z|\chi_1\rangle + 2b(\epsilon A')^2\mathcal{L}u_{as}\partial_{zz}|\chi_1\rangle \\ &- 3(\epsilon A')^2\mathcal{L}u_{as}u_{ls}|\chi_1\rangle.\end{aligned}$$

The application of the solvability condition at the next order leads to

$$\dot{A}' = \frac{2c_0\langle\psi_1|\mathcal{L}\partial_z u_{as}|\chi_0\rangle}{\langle\psi_1|\chi_0\rangle}A' - \frac{\langle\psi_1|\mathcal{L}u_{as}^2|\chi_1\rangle}{\langle\psi_1|\chi_0\rangle}A'^3. \tag{8}$$

To simplify further Eqs. (7) and (8), we propose the following scaling and change of parameters:

$$A \equiv \frac{\langle\psi_1|\mathcal{L}u_{as}^2|\chi_1\rangle}{\langle\psi_1|\chi_0\rangle}A', \quad \tau \equiv \frac{\langle\psi_1|\chi_0\rangle}{\langle\psi_1|\mathcal{L}u_{as}^2|\chi_1\rangle}t, \tag{9}$$

$$\sigma \equiv 2c_0\frac{\langle\psi_1|\mathcal{L}\partial_z u_{as}|\chi_0\rangle\langle\psi_1|\mathcal{L}u_{as}^2|\chi_1\rangle}{\langle\psi_1|\chi_0\rangle^2},$$

we get the dynamics for the critical modes

$$\dot{A}(\tau) = \sigma A - A^3, \tag{10}$$

$$\dot{x}_0(\tau) = -A. \tag{11}$$

The parameter $\sigma \propto (c - c^*)$ measures the distance from the critical point associated with the parity symmetry breaking transition. The stationary speed of amplitude Eqs. (10) and (11) is $v = \pm\sqrt{\sigma} \propto (c - c^*)^{1/2}$. This implies that the asymmetric mode undergoes at the onset of the instability a drift-pitchfork bifurcation,[35,36] as result of parity breaking symmetry.[19,20,26,30,33] This bifurcation scenario is in perfect agreement with the results of direct numerical simulations of Eq. (1) presented in Sec. II [see the bifurcation diagram of Fig. 1]. Note that the interaction between symmetric stationary LSS has been investigated in the variational Swift-Hohenberg equation by Aranson *et al.*[36]

IV. BOUNDED MOVING LOCALIZED STATES IN TWO SPATIAL DIMENSIONS

Most of the experimental observations of localized structures have been realized in two-dimensional systems,[4,5] in which stationary localized structures are observed. Experimentally, it has been reported a supercritical transition from stationary to moving localized structures in a planar gas-discharge system.[33]

An example of two-dimensional moving localized states obtained by numerical simulations of Eq. (1) is depicted in Fig. 5(a). In this figure, a time sequence of two-dimensional moving bounded states obtained for periodic boundary conditions is shown. The two spots are bounded together in the course of the motion. The nonvariational effects render this localized moving spots asymmetric. There is no preferred direction for this motion since the system is isotropic in the xy plane. We characterize this motion by computing the speed ($\dot{x}_0$) as a function of the nonvariational parameter c. The result is shown in Fig. 5(b). The existence domain of this moving structures occurs in the range of $c_1 < c < c_2$. For $c < c_1$, the system undergoes a well documented curvature instability that affects the circular shape of LS and in the course of time leads to a self-replication phenomena.[37] This behaviour is illustrated in Fig. 6(a). However, for $c > c_2$, bounded localized structures become unstable and we observe in this regime transition to homogeneous steady state as shown in Fig. 6(b).

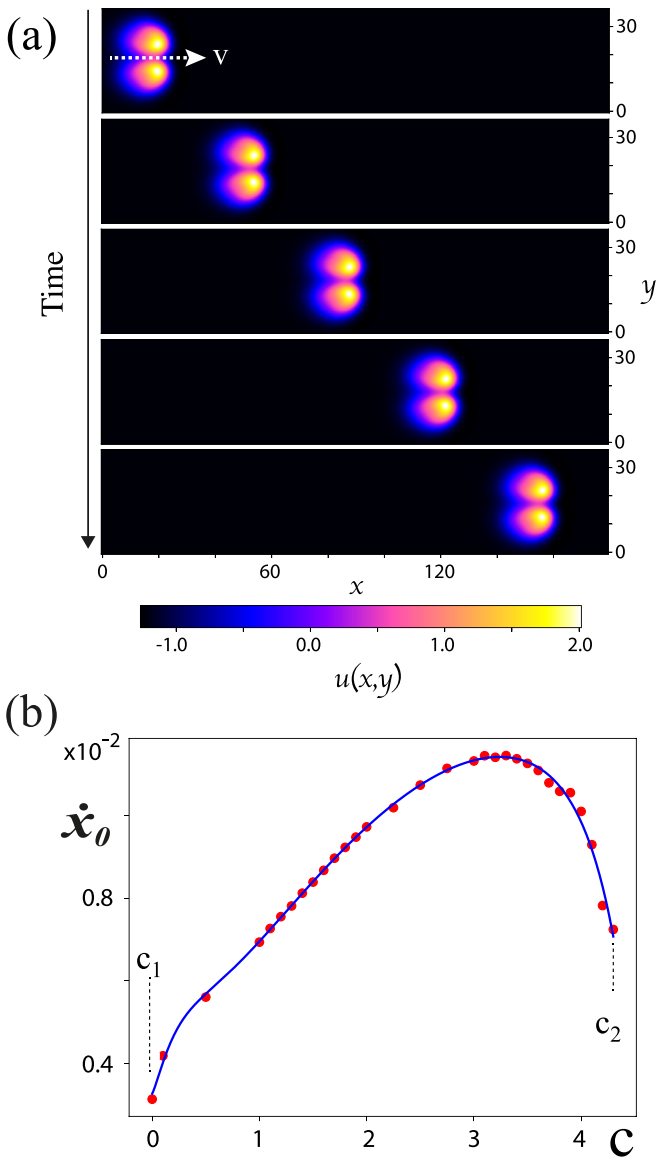

FIG. 5. Moving bounded localized structures obtained from numerical simulations of Eq. (1). (a) Temporal sequence of the moving bounded LSs in (x, y) plane obtained at $t_1 = 0$, $t_2 = 1500$, $t_3 = 3000$, $t_4 = 4500$, and $t_5 = 6000$ time steps. Parameters are $\eta = -2$, $\nu = -1$, $\mu = -0.092$, $b = -2.8$, and $c = 3.2$. (b) The speed of bounded moving LSs as a function of the parameter c. Other parameters are the same as in (a). The red dots indicate localized structures speed obtained from numerical simulations of Eq. (1) and the blue curve shows an interpolation obtained from these dots.

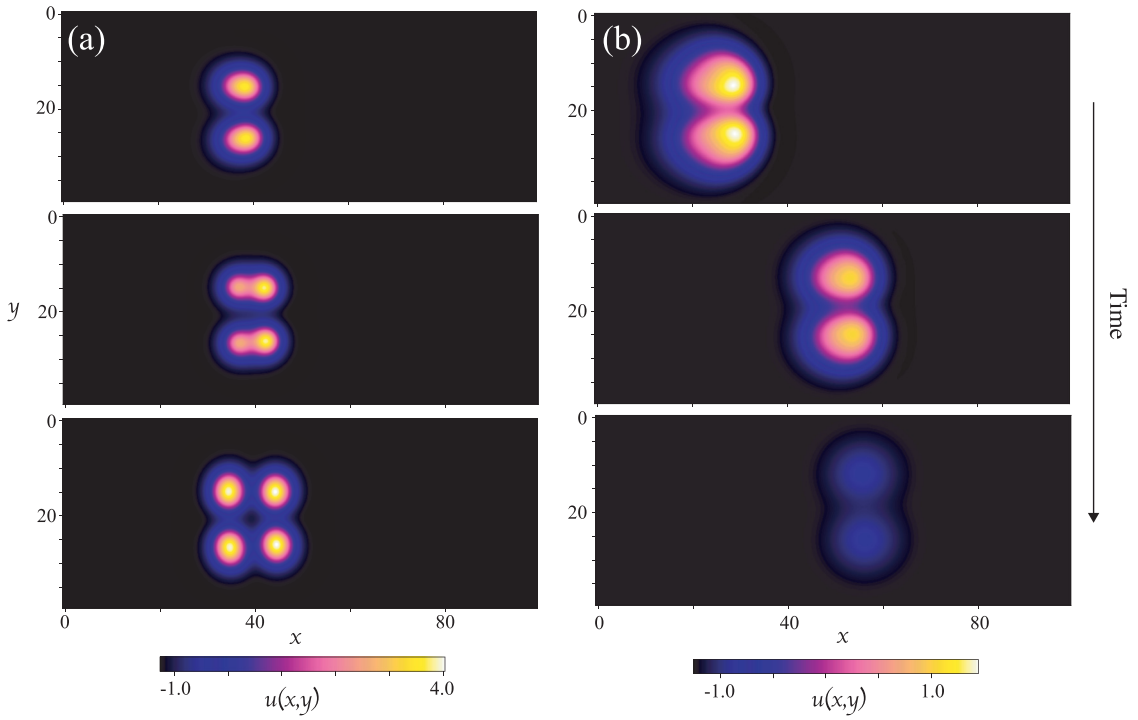

FIG. 6. Temporal sequence of destabilization of bounded localized structures via (a) a self-replication or (b) a transition towards stationary homogeneous steady states. Parameters are the same as in Fig. 5 except for c, (a) $c=-0.2$ and (b) $c=4.5$.

V. CONCLUSION

We have considered the paradigmatic real nonvariational Swift-Hohenberg equation with cubic nonlinearity. We have investigated the transition from stable stationary to moving localized structures. We have shown that the spontaneous motion of localized structures induced by parity symmetry transition and nonvariational effects is supercritical and occurs in wide range of the system parameter values. In one dimensional setting, the analytical and the numerical bifurcation diagrams have been established. We have derived a normal form equation to describe the amplitude and the speed of moving localized structures. We have estimated the threshold as well as the speed of moving asymmetric localized structures. A similar scenario has been established for cubic-quintic Swift-Hohenberg equation with only the nonvariational nonlinear advective term.[38] In this paper, a drift pitchfork bifurcation of localized states has been discussed where the resulting traveling states are linearly stable. However, in two-dimensional systems, we have shown through numerical simulations that the transition towards bounded moving localized state is rather subcritical. We have shown that there exist a finite range of parameters where bounded LS is stable. Out of this parameter range, the 2D bounded localized state self-replicates or exhibits transition towards a stationary homogeneous steady state.

Our results are valid in the double limits of a critical point associated with nascent bistability and close to short wavenumber or large wavelength pattern forming regime. However, given the universality of model (1), we expect that the transition considered here should be observed in various far from equilibrium systems.

ACKNOWLEDGMENTS

M.G.C. and M.T. acknowledge the support of CONICYT Project No. REDES-150046. M.T. received support from the Fonds National de la Recherche Scientifique (Belgium). M.G.C. thanks FONDECYT Project No. 1150507 and Millennium Institute for Research in Optics. A.J.A.-S. thanks financial support from Becas Conicyt 2015, Contract No. 21151618.

[1]P. Glansdorff and I. Prigogine, *Thermodynamic Theory of Structures, Stability and Fluctuations* (Wiley, New York, 1971).
[2]M. C. Cross and P. C. Hohenberg, "Pattern formation outside of equilibrium," Rev. Mod. Phys. **65**, 851 (1993).
[3]*Dissipative Solitons: From Optics to Biology and Medicine*, Lecture Notes in Physics Vol. 751, edited by N. Akhmediev and A. Ankiewicz (Springer, Heidelberg, 2008).
[4]H. G. Purwins, H. U. Bodeker, and S. Amiranashvili, "Dissipative solitons," Adv. Phys. **59**, 485 (2010).
[5]O. Descalzi, M. G. Clerc, S. Residori, and G. Assanto, *Localized States in Physics: Solitons and Patterns* (Springer, 2011).
[6]H. Leblond and D. Mihalache, Phys. Rep. **523**, 61 (2013).
[7]M. Tlidi, K. Staliunas, K. Panajotov, A. G. Vladimiorv, and M. Clerc, Philos. Trans. R. Soc., A **372**, 20140101 (2014).
[8]L. Lugiato, F. Prati, and M. Brambilla, *Nonlinear Optical Systems* (Cambridge University Press, 2015).
[9]*Nonlinear Dynamics: Materials, Theory and Experiments*, Springer Proceedings in Physics Vol. 173, edited by M. Tlidi and M. G. Clerc (Springer, 2016).
[10]M. E. Cates, D. Marenduzzo, I. Pagonabarraga, and J. Tailleur, Proc. Natl. Acad. Sci. U. S. A. **107**, 11715 (2010).
[11]D. Turaev, M. Radziunas, and A. G. Vladimirov, Phys. Rev. E **77**, 065201(R) (2008).
[12]R. Zambrini and F. Papoff, Phys. Rev. Lett. **99**, 063907 (2007).
[13]K. Staliunas and V. J. Sanchez-Morcillo, Phys. Rev. A **57**, 1454 (1998).
[14]F. Haudin, R. G. Rojas, U. Bortolozzo, M. G. Clerc, and S. Residori, Phys. Rev. Lett. **106**, 063901 (2011).

[15]P. V. Paulau, D. Gomila, T. Ackemann, N. A. Loiko, and W. J. Firth, Phys. Rev. E **78**, 016212 (2008).
[16]A. J. Scroggie, W. J. Firth, and G.-L. Oppo, Phys. Rev. A **80**, 013829 (2009).
[17]M. Tlidi, A. G. Vladimirov, D. Pieroux, and D. Turaev, Phys. Rev. Lett. **103**, 103904 (2009).
[18]S. V. Gurevich and R. Friedrich, Phys. Rev. Lett. **110**, 014101 (2013).
[19]P. Coullet, J. Lega, B. Houchmanzadeh, and J. Lajzerowicz, Phys. Rev. Lett. **65**, 1352 (1990).
[20]J. Burke and E. Knobloch, Chaos **17**, 037102 (2007).
[21]M. G. Clerc, A. Petrossian, and S. Residori, Phys. Rev. E **71**, 015205(R) (2005).
[22]C. Durniak, M. Taki, M. Tlidi, P. L. Ramazza, U. Bortolozzo, and G. Kozyreff, Phys. Rev. E **72**, 026607 (2005).
[23]G. Kozyreff, S. J. Chapman, and M. Tlidi, Phys. Rev. E **68**, 015201(R) (2003).
[24]G. Kozyreff and M. Tlidi, Chaos **17**, 037103 (2007).
[25]M. Tlidi, P. Mandel, and R. Lefever, Phys. Rev. Lett. **73**, 640 (1994).
[26]J. Burke and J. H. Dawes, SIAM J. Appl. Dyn. Syst. **11**, 261 (2012).
[27]M. Tlidi, E. Averlant, A. Vladimirov, and K. Panajotov, Phys. Rev. A **86**, 033822 (2012).
[28]D. Michaelis, U. Peschel, F. Lederer, D. Skryabin, and W. J. Firth, Phys. Rev. E **63**, 066602 (2001).
[29]J. M. Gilli, M. Morabito, and T. Frisch, J. Phys. II France **4**, 319–331 (1994).
[30]M. G. Clerc, S. Coulibaly, and D. Laroze, Int. J. Bifurcation Chaos Appl. Sci. Eng. **19**, 2717 (2009).
[31]A. Esteban-Martín, V. B. Taranenko, J. García, G. J. de Valcárcel, and E. R. Eugenio, Phys. Rev. Lett. **94**, 223903 (2005).
[32]A. J. Alvarez-Socorro, M. G. Clerc, M. Gonzelez-Cortes, and M. Wilson, Phys. Rev. E **95**, 010202 (2017).
[33]H. U. Bödeker, M. C. Röttger, A. W. Liehr, T. D. Frank, R. Friedrich, and H. G. Purwins, Phys. Rev. E **67**, 056220 (2003).
[34]I. Fredholm, Acta Math. **27**, 365 (1903).
[35]S. Wiggins, *Introduction to Applied Nonlinear Dynamical Systems and Chaos* (Springer-Verlag, New York, 1990).
[36]I. S. Aranson, K. A. Gorshkov, A. S. Lomov, and M. I. Rabinovich, Phys. D **43**, 435 (1990).
[37]I. Bordeu *et al.*, Sci. Rep. **6**, 33703 (2016).
[38]S. M. Houghton and E. Knobloch, Phys. Rev. E **84**, 016204 (2011).